J. C. Bose Journal of Engineering, Technology and Sciences
Vol. 2, Issue No. 1, October 2026

Voltage Dependence of Pulse Shape Properties and Dead Time of a Geiger-Müller Counter

Vikas Kumar[1], Ankit Kumar[1], Vikas[1], Aryan[1], Kajal[1] and Hardev Singh[1*]

[1]Department of Physics, Kurukshetra University, Kurukshetra, Haryana – 136119, India

Abstract: Accurate determination of the dead time of a Geiger–Müller (GM) counter is crucial for reliable radiation counting, particularly in applications requiring precise rate corrections. Although GM counters are commonly operated within the plateau region, a systematic understanding of how operating voltage influences dead time and associated pulse shape characteristics remains limited. In this work, we investigate the voltage dependence of the dead time and pulse shape parameters of a GM counter operated in the plateau region. The dead time was determined using the standard two-source method under the assumption of a non-paralyzing model, employing radioactive sources ^{60}Co and ^{137}Cs. Pulse shape characteristics, including pulse width, fall time, and peak-to-peak voltage, were measured using a digital oscilloscope. The results show a clear decrease in dead time with increasing operating voltage. Strong correlations are observed between dead time and pulse shape parameters, where longer pulse widths and fall times correspond to larger dead times at lower operating voltages. In the low-voltage region, the extended electron collection time at the anode enhances charge recombination, resulting in increased dead time and broader pulse width. With increasing voltage, faster charge collection reduces fall time and pulse width, leading to shorter dead time. These findings quantitatively establish the interdependence of dead time, operating voltage, and pulse shape characteristics, providing insights for optimizing GM counter operation and improving counting accuracy.

Keywords: *GM counter, Dead-time, Radioactive sources*

1. Introduction

Radiation or particle detectors are devices used to measure ionization produced by different types of ionizing radiation such as alpha, beta, gamma rays, and X-rays. Depending on the nature and energy of the radiation, various detector types such as solid-state, scintillation, and gas-filled detectors are employed. Among gas-filled detectors, the Geiger–Müller (GM) counter remains one of the most widely used instruments due to its simplicity, robustness, low cost, and ability to detect a broad range of ionizing radiations.

The GM counter, originally developed by Hans Geiger and Walther Müller in 1928 (Geiger, Müller, et al., 1928), is one of the earliest radiation detection devices and continues to play an important role in nuclear physics, radiation protection, and health physics. Its long-standing relevance arises from its straightforward design, ease of operation, and reliable response, making it a fundamental tool for both laboratory experiments and field measurements. A detailed understanding of its operational characteristics is therefore essential for ensuring accurate radiation counting and detector optimization.

The GM counter operates as a gas-filled detector based on the principle of gas multiplication. When ionizing radiation enters the detector volume, it produces electron–positive ion pairs through direct ionization (in the case of alpha and beta particles) or indirect ionization (for gamma rays and X-rays). Under the influence of a strong applied electric field, electrons drift rapidly toward the anode wire while the heavier positive ions move toward the cathode. The energetic electrons initiate secondary ionization processes,

*Corresponding author
Email address: hsinghphy@kuk.ac.in

Received 13 May 2025; Accepted 04 April 2026
Published online 11 October 2026

©2026 JCBJETS

and excited gas atoms emit photons that further contribute to ionization. This sequence of processes leads to the formation of a Townsend avalanche, resulting in a detectable electrical pulse (Knoll, 2010).

Under suitable operating conditions, a single avalanche can trigger a self-propagating discharge that spreads along the anode wire and encompasses the entire detector volume. As a result, all pulses generated in a GM counter have nearly identical amplitudes and shapes, independent of the type or energy of the incident radiation. The electrons produced in the avalanche are collected rapidly at the anode, while the slower-moving positive ions form a space-charge sheath around the anode wire. This ion sheath temporarily distorts the local electric field and influences the charge collection process (Knoll, 2010).

Because positive ions drift much more slowly than electrons, their accumulation near the anode prolongs the recovery time of the detector. During this interval, subsequent radiation events may not be registered, leading to a phenomenon known as dead time (Knoll, 2010; Akyurek, Yousaf, Liu, & Usman, 2015; Stever, 1942). Dead time is defined as the minimum time interval required for two successive radiation events to be recorded as independent counts. Events occurring within this interval are lost, which directly affects the accuracy of measured count rates, especially at higher radiation intensities (Müller, 1973).

Among the key parameters governing the performance of a GM counter are its pulse shape characteristics, including pulse width, fall time, peak-to-peak voltage, and dead time. These parameters are strongly influenced by detector operating conditions such as applied voltage, gas composition, pressure, and temperature. Although the dead time of GM counters has been widely studied using standard methods, systematic experimental investigations linking dead time with voltage-dependent pulse shape properties in the plateau region remain limited. In particular, a quantitative correlation between pulse width, fall time, and dead time as a function of operating voltage has not been sufficiently explored.

The present work aims to provide a comprehensive experimental study of the voltage dependence of pulse shape properties and dead time of a GM counter operated in the plateau region. The dead time is measured using the standard two-source method, while pulse shape parameters are extracted using a digital oscilloscope. In this work, we performed a systematic measurement of the dead time as a function of operating voltage and carried out a detailed analysis of pulse width, fall time, and peak-to-peak voltage with changing voltage to establish a clear correlation between pulse shape characteristics and dead time.

2. Dead Time Models

Dead time is an inherent characteristic of radiation counting systems and plays a critical role in determining the accuracy of measured count rates. To describe dead time behavior, two idealized models are commonly employed: the paralyzing model and the non-paralyzing model.

The paralyzing dead time model, also referred to as the extending type model, was first proposed by W. Feller (Feller, 1948). In this model, once a radiation event is detected, the system becomes insensitive for a fixed dead time interval. Any additional radiation event occurring within this interval not only goes unrecorded but also resets the dead time, thereby extending the paralysis period. As a result, the detector remains continuously paralyzed until a time interval equal to or greater than the dead time elapses without any radiation interaction. The relationship between the observed count rate m and the true count rate n for the paralyzing model is given by (Feller, 1948):

$$m = n \exp(-n\tau), \tag{1}$$

where τ is the detector dead time. This model represents a lower limiting case for detector response and is most applicable to systems in which successive events strongly interfere with charge recovery.

In contrast, the non-paralyzing dead time model, introduced by R. D. Evans (Evans, 1955), assumes that radiation events occurring during the dead time are simply lost without affecting the duration of the dead time itself. In this case, the detector resumes normal operation after a fixed dead time following each registered event. The corresponding relationship between the observed and true count rates is expressed as (Evans, 1955):

$$m = \frac{n}{1 + n\tau}. \tag{2}$$

The non-paralyzing model represents an upper limiting case of dead time behavior and is often considered a good approximation for Geiger–Müller (GM) counters operating under typical conditions.

Since real detectors do not strictly follow either of these idealized models, hybrid dead time models have been proposed to better represent experimental observations. One such model was developed by Lee and Gardner (Lee & Gardner, 2000), which incorporates both paralyzing and non-paralyzing dead time components into a single analytical expression:

$$m = \frac{n \exp(-n\tau_p)}{1 + n\tau_{np}}, \tag{3}$$

where τ_p and τ_{np} represent the paralyzing and non-paralyzing dead times, respectively. Another hybrid approach was proposed by Patil and Usman (Patil & Usman, 2009), who introduced a paralysis factor f to interpolate between the two limiting cases:

$$m = \frac{n \exp(-fn\tau)}{1 + (1 - f)n\tau}. \tag{4}$$

In this formulation, the hybrid model reduces to the paralyzing model when $f = 1$ and to the non-paralyzing model when $f = 0$.

Experimental validation of hybrid dead time models using the decaying source method with ^{56}Mn has shown that the paralysis factor for GM counters is typically 5% or lower, indicating predominantly non-paralyzing behavior (Akyurek et al., 2015; Evans, 1955; Almutairi, Alam, Akyurek, Goodwin, & Usman, 2020). This observation justifies the widespread assumption of the non-paralyzing model for GM counters in practical applications.

Accordingly, in the present study, dead time measurements were performed using the two-source method under the assumption of non-paralyzing behavior. The variation of dead time with operating voltage in the plateau region was systematically investigated. Furthermore, the observed trends in dead time were corroborated through a detailed analysis of voltage-dependent pulse shape parameters. The results of this study provide additional experimental verification of earlier findings reported by Almutairi et al.(Almutairi, Alam, Goodwin, Usman, & Akyurek, 2021; Almutairi, Akyurek, & Usman, 2019) using ^{60}Co and ^{137}Cs radioactive sources.

3. Experimental Details

The present experimental investigations were carried out in the Nuclear Physics Laboratory, Department of Physics, Kurukshetra University, Kurukshetra, to study the voltage dependence of pulse shape characteristics and dead time of a Geiger–Müller (GM) counter operated in the plateau region. Radioactive sources of cesium-137 (^{137}Cs) and cobalt-60 (^{60}Co) were used for pulse shape analysis and dead time measurements. The ^{137}Cs source emits a single discrete gamma ray of energy 0.661 MeV, whereas the ^{60}Co source emits two discrete gamma rays with energies of 1.1732 MeV and 1.3325 MeV. Both radioactive sources employed in the present study had identical physical dimensions and geometry to ensure uniform irradiation conditions and to minimize systematic uncertainties during measurements.

Radiation detection and counting were performed using a Geiger counting system (AT type: GC601A) manufactured by NUCLEONIX Systems Pvt. Ltd.. The counting system is based on an 8-bit micro controller and is equipped with a 20 $\times$ 2 LCD dot-matrix display for real-time monitoring of counts and elapsed time. It provides a variable extra-high tension (EHT) supply in the range of 0–1500 V, with a maximum counting capacity of 999999 counts and a programmable preset counting time of up to 9999 s. The detector used in this work was a halogen-quenched, end-window Geiger–Müller tube with dimensions of approximately 3.3 cm in length and 1.5 cm in diameter.

Pulse shape measurements were carried out using a digital storage oscilloscope (DSO), model GDS-1102-U, manufactured by GW Instek. The GM tube was connected to the Geiger counting system using a coaxial cable, and the output signal was simultaneously fed to the oscilloscope for pulse shape analysis. The oscilloscope was operated in its automatic measurement mode to determine pulse width, fall time, and peak-to-peak voltage from the recorded pulse trains. Representative pulse waveforms were stored directly via a USB interface for further analysis.

Dead time measurements were performed using the standard two-source method under the assumption of non-paralyzing detector behavior. Individual count rates were measured for each radioactive source separately as well as for the combined sources at different operating voltages within the plateau region of the GM counter. The dead time at each operating voltage was calculated from the measured count rates, and the observed variation of dead time with voltage was correlated with the corresponding changes in pulse shape parameters.

4. Results and Discussion

The primary objective of the present study is to investigate the variation of the dead time of a Geiger–Müller (GM) counter as a function of operating voltage. To identify the appropriate operating voltage range of the GM tube, the plateau region was first determined by measuring the count rate as a function of applied voltage using a ^{137}Cs radioactive source. The resulting count rate–voltage characteristic, which defines the plateau region of the GM counter, is shown in Figure. 1.

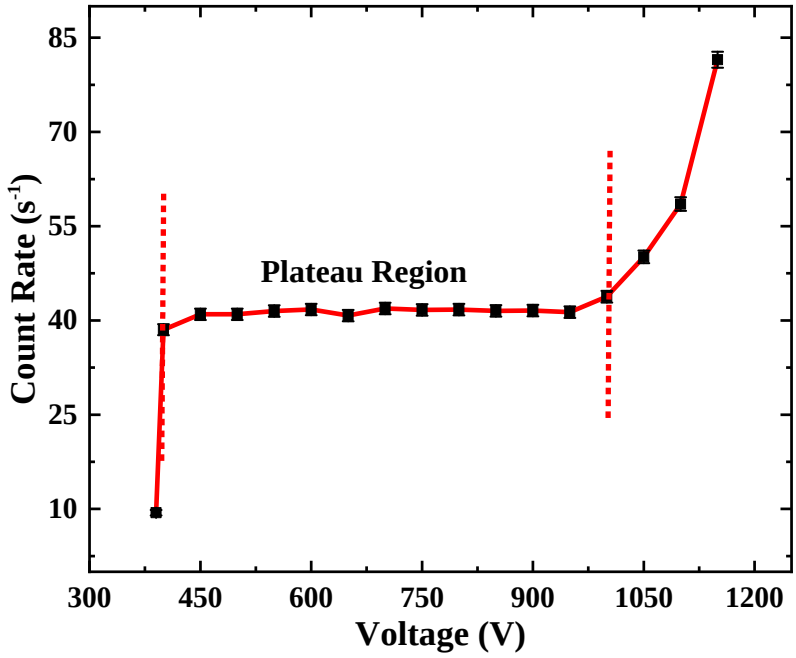


Figure 1: Variation of count rate as a function of applied voltage (filled squares) for the Geiger–Müller counter using a ^{137}Cs source. The voltage range bounded by the two vertical dotted lines represents the plateau region of the GM tube. The continuous red line joining the data is to guide the eye.

To investigate the dead time of the Geiger–Müller (GM) counter and its dependence on the applied operating voltage, the well-established two-source method was employed. This method is based on measuring the counting rates from two radioactive sources individually and in combination. Owing to the nonlinear nature of counting losses, the observed counting rate from the combined sources is lower than the sum of the individual counting rates. This difference provides a measure of the detector dead time.

Accordingly, the dead time was evaluated at each applied voltage using the non-paralyzing model and calculated using the following relation (Knoll, 2010),

$$\tau = \frac{s_1 + s_2 - s_{12}}{2 s_1 s_2}\, \tau_n, \tag{5}$$

where s_1 and s_2 are the measured count rates obtained using source 1 and source 2, respectively, s_{12} is the measured count rate with both sources present, τ_n is the measuring time (200 s in the present study), and τ denotes the detector dead time. In addition, the dead time was also determined using an alternative formulation (Knoll, 2010; Evans, 1955),

$$\tau = \frac{X\left(1 - \sqrt{1 - Z}\right)}{Y} \tag{6}$$

where $X = s_1 s_2 - s_b s_{12}$, $Y = s_1 s_2 \left(s_{12} + s_b\right) - s_b s_{12} \left(s_1 + s_2\right)$ and $Z = \frac{Y(s_1 + s_2 - s_{12} - s_b)}{X^2}$,

Here, s_b represents the background count rate. The dead time values obtained from Eqs. (5) and (6) were found to be in close agreement. Therefore, the dead time values reported in this work are those calculated using Eq. (5).

Although the non-paralyzing model is assumed in the present analysis, this assumption is justified by the close agreement observed between dead time values obtained using two independent non-paralyzing formulations, namely Eqs. (5) and (6). Such agreement indicates that paralyzing effects, if present, are negligible under the operating conditions employed in this study, which is consistent with earlier reports for GM counters operated in the plateau region (Evans, 1955; Almutairi et al., 2019). Furthermore, earlier studies have indicated the negligible contribution (5%) fraction of paralyzing dead time to the overall measured dead time (Akyurek et al., 2015; Evans, 1955; Almutairi et al., 2020).

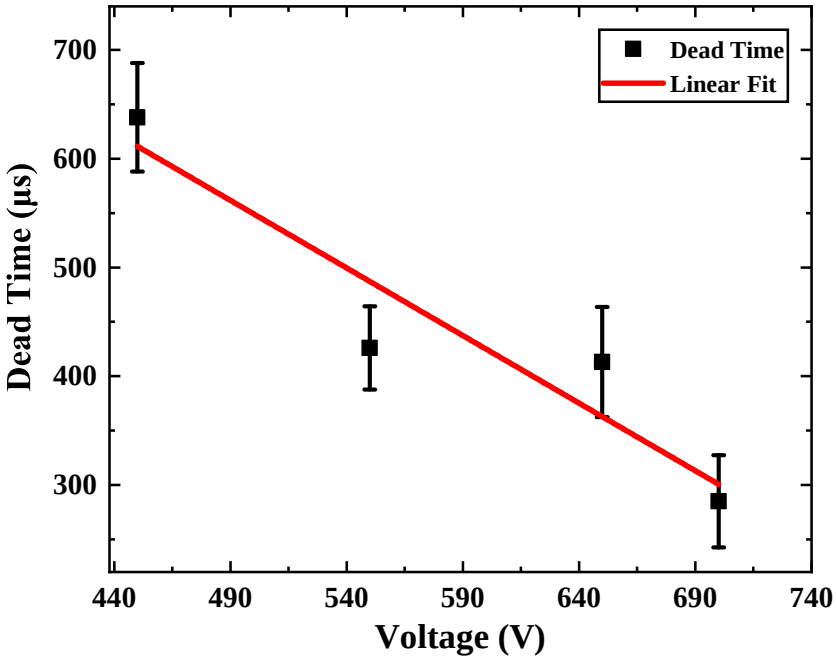


Figure 2: Variation of the dead time with applied operating voltage measured using the ^{137}Cs source. The red line is a linear fit to the data.

Since the two-source method involves evaluating the difference between nearly equal count rates, careful experimental procedures were followed to ensure reliable results. The radioactive sources were kept

fixed throughout the measurements to avoid geometrical variations. To maintain identical scattering conditions, a dummy source without activity was placed in position when counting each source individually.

Dead time measurements were carried out at four different operating voltages within the plateau region of the Geiger–Müller (GM) tube. For each voltage, the reported dead time represents the average of three independent measurements. The variation of dead time with applied voltage is shown in Figure. 2.

To further investigate the origin of the observed dead time behavior, pulse shape measurements were performed using a digital storage oscilloscope. In this experiment, background radiation was initially detected by the GM counter, and the operating voltage was set to 360 V, corresponding to the onset of detectable pulses. The voltage was then increased in steps of 20 V up to 600 V. At each voltage, pulse waveforms were recorded using the oscilloscope's run/stop mode.

Pulse shape parameters, including pulse width, fall time, and peak-to-peak voltage, were extracted using the oscilloscope's automatic measurement feature. For each voltage, three independent observations were performed to ensure reproducibility. The correlation between pulse shape characteristics and dead time variation is discussed in the following subsections.

4.1. Peak-to-Peak Voltage

Peak-to-peak voltage (V_{pp}) is defined as the absolute difference between the maximum and minimum amplitudes of an output pulse. Measurements of V_{pp} were carried out for the ^{60}Co and ^{137}Cs radioactive sources, as well as for background radiation. The corresponding results are presented in Figures. 3–5.

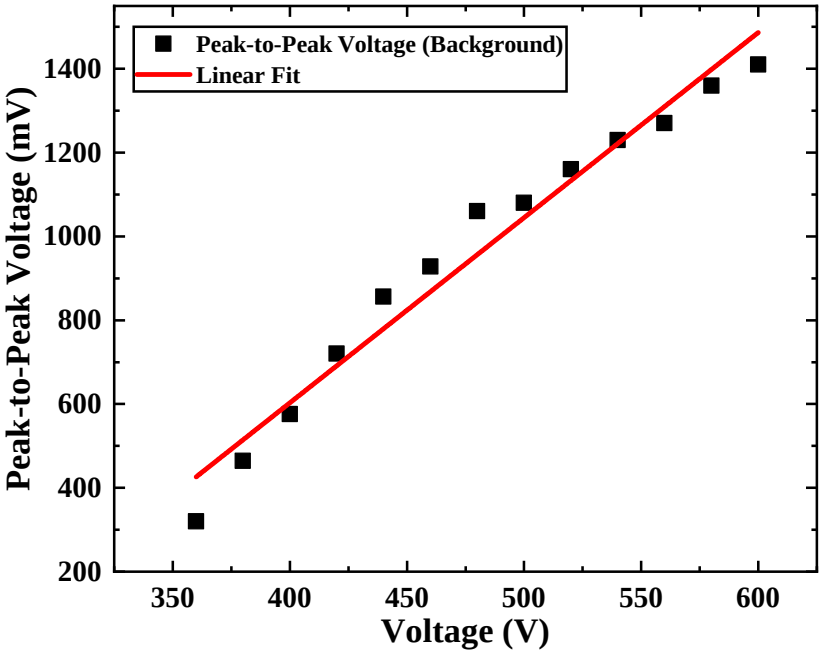


Figure 3: Variation of peak-to-peak voltage (V_{pp}) with applied voltage for background radiation. The red line represents a linear fit to the experimental data. The trend illustrates a linear increase in pulse amplitude with voltage reflecting the enhanced charge collection and gain in the GM counter.

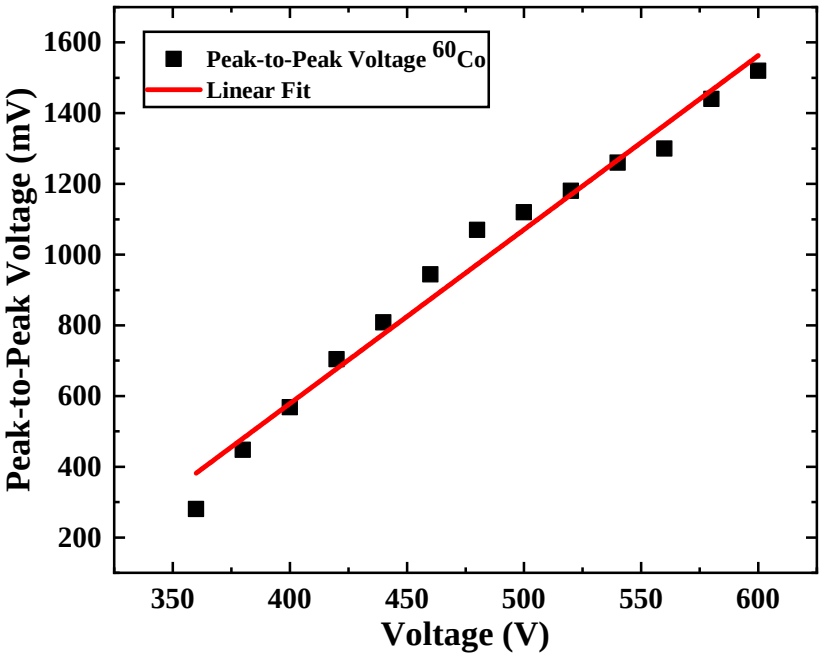


Figure 4: Variation of peak-to-peak voltage (V_{pp}) with applied voltage for the ^{60}Co radioactive source. The red line represents a linear fit to the measured data.

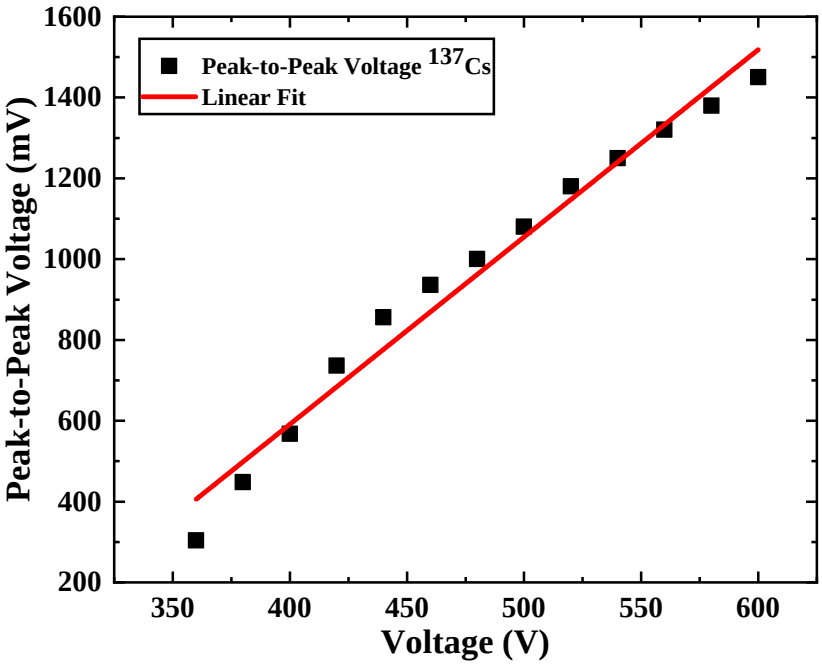


Figure 5: Variation of peak-to-peak voltage (V_{pp}) as a function of applied voltage for the ^{137}Cs source. The red line represents the linear fit to the experimental data.

For both radioactive sources and background radiation, the measured V_{pp} values are found to be consistent, reflecting the characteristic operating behavior of a Geiger–Müller (GM) tube. In a GM counter,

the pulse amplitude is largely independent of the number of primary ion pairs created or the energy of the incident radiation, owing to complete gas multiplication during the discharge process.

The variation of V_{pp} with applied voltage exhibits an approximately linear increase over the studied voltage range (see Figures. 3–5). This behavior is attributed to enhanced charge collection efficiency and increased gain with rising operating voltage. The extracted rates of change of V_{pp} with voltage are 4.92 ± 0.22 mV/V for the ^{60}Co source, 4.65 ± 0.22 mV/V for the ^{137}Cs source, and 4.42 ± 0.24 mV/V for background radiation. The close agreement among these values further confirms the voltage-dependent yet radiation-independent pulse amplitude response of the GM counter.

4.2. Pulse Width

Pulse width is defined as the time interval between the points on the rising and falling edges of a pulse corresponding to 50% of its maximum amplitude. Pulse width measurements were performed for background radiation as well as for the ^{60}Co and ^{137}Cs radioactive sources. The measured pulse width data for all three cases are presented in Figures. 6–8.

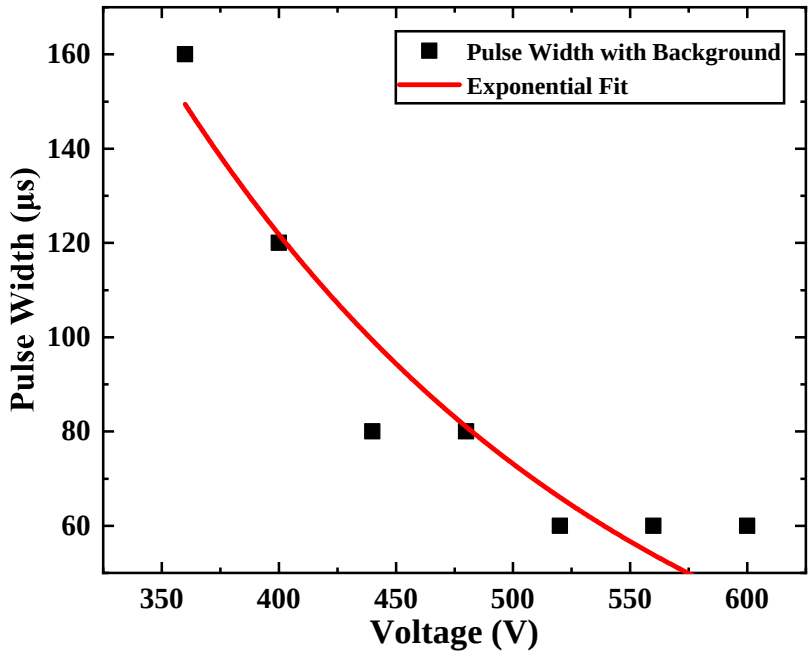


Figure 6: Variation of pulse width with applied voltage for the background radiation. Red line represents the exponential fit to the measured data, illustrating the decrease in pulse width with increasing voltage.

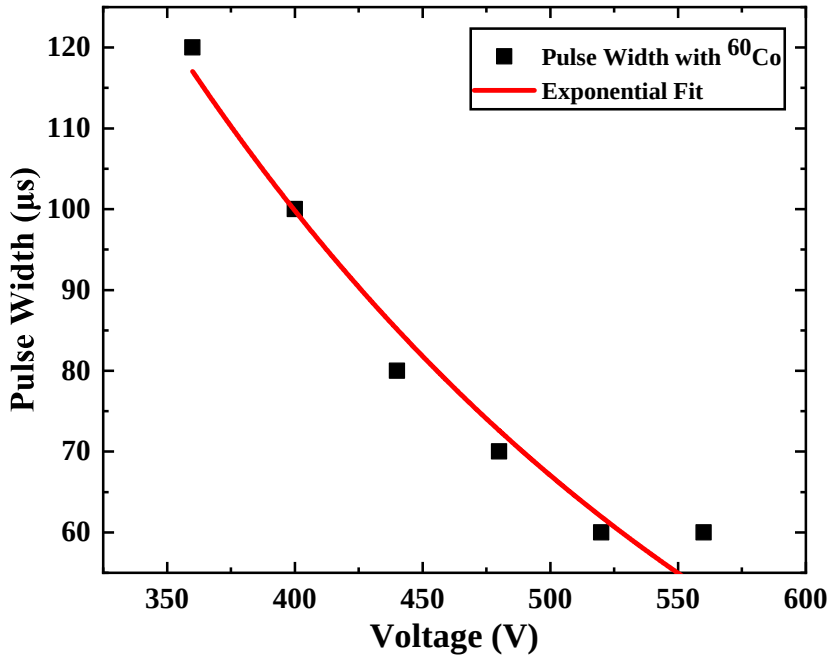


Figure 7: Variation of pulse width with applied voltage for the ^{60}Co source. The red line represents the exponential fit to the measured data, illustrating the decrease in pulse width with increasing voltage.

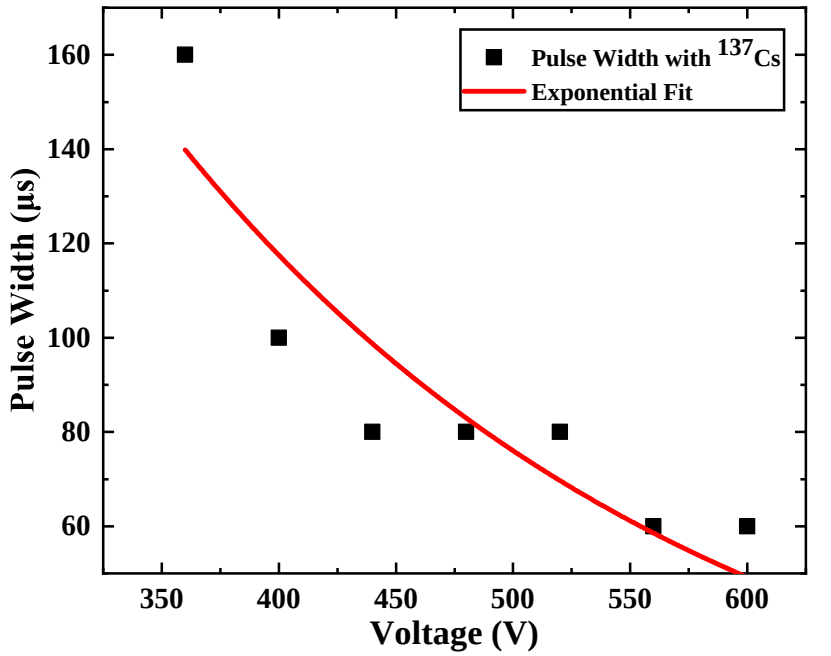


Figure 8: Variation of pulse width with applied voltage for the ^{137}Cs source. The red line represents the exponential fit to the measured data, illustrating the decrease in pulse width with increasing voltage.

The variation of pulse width with applied voltage exhibits a similar trend for background radiation and both radioactive sources. As shown in Figures. 6–8, the pulse width decreases exponentially with increas-

ing operating voltage and attains its maximum value at lower voltages. At low electric field strengths, the ionization and charge collection processes are relatively slow, leading to broader pulses. With an increase in the applied voltage, the electric field strength inside the detector increases, enhancing the development of Townsend avalanches and accelerating charge collection. Consequently, the detected pulses become narrower. To quantify this behavior, the pulse width data were fitted using an exponential function of the form $a\exp(-bV)$, where V is the applied voltage. The fitted curves are represented by solid red lines in Figures. 6–8, and the corresponding best-fit parameters are summarized in Table 1. The extracted exponent values are 0.00510 for background radiation, 0.00397 for the ^{60}Co source, and 0.00435 for the ^{137}Cs source. Although the exponent for background radiation is slightly higher than those for the radioactive sources, the overall voltage dependence of pulse width remains comparable for all three cases. Among the studied sources, the pulse width data for the ^{60}Co source exhibit the best agreement with the exponential fit.

Table 1: Best-fit parameters (a and b) obtained from exponential fitting of the pulse width as a function of applied voltage for background radiation and the radioactive sources ^{60}Co and ^{137}Cs.

S. No.	Source	a	b
1	Background	939.94 ± 309.50	0.00510 ± 0.00077
2	^{60}Co	490.23 ± 80.34	0.00397 ± 0.00038
3	^{137}Cs	670.59 ± 274.00	0.00435 ± 0.00094

4.3. Fall Time

Fall time (pulse decay time) is defined as the time required for the pulse amplitude to decrease from 90% to 10% of its peak value, excluding any overshoot or undershoot. The fall time was determined manually from the recorded pulse shapes at different operating voltages. The variation of fall time with applied voltage for the ^{60}Co, ^{137}Cs, and background radiation measurements is presented in Figures. 9–11.

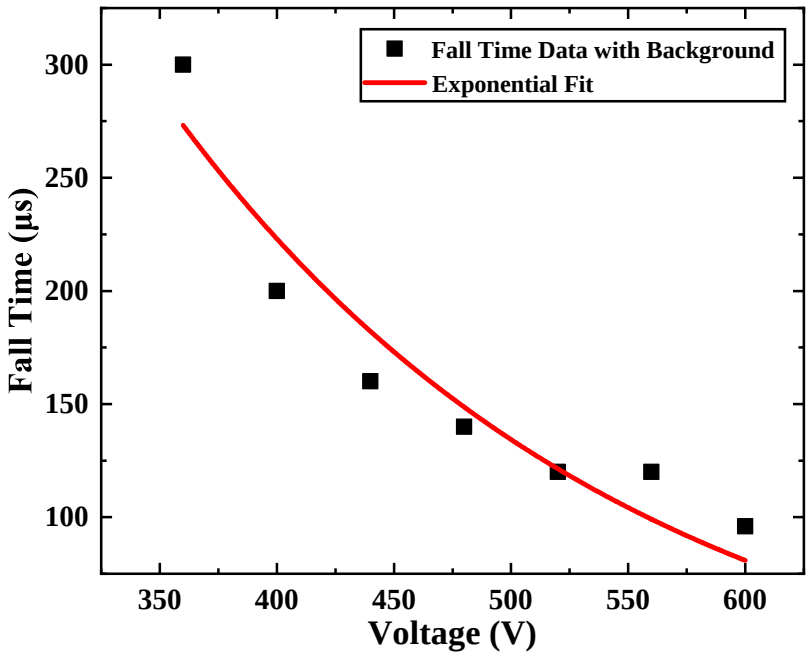


Figure 9: Variation of fall time with applied voltage for background radiation. The red line represents the exponential fit to the measured data, illustrating the decrease in fall time with increasing voltage.

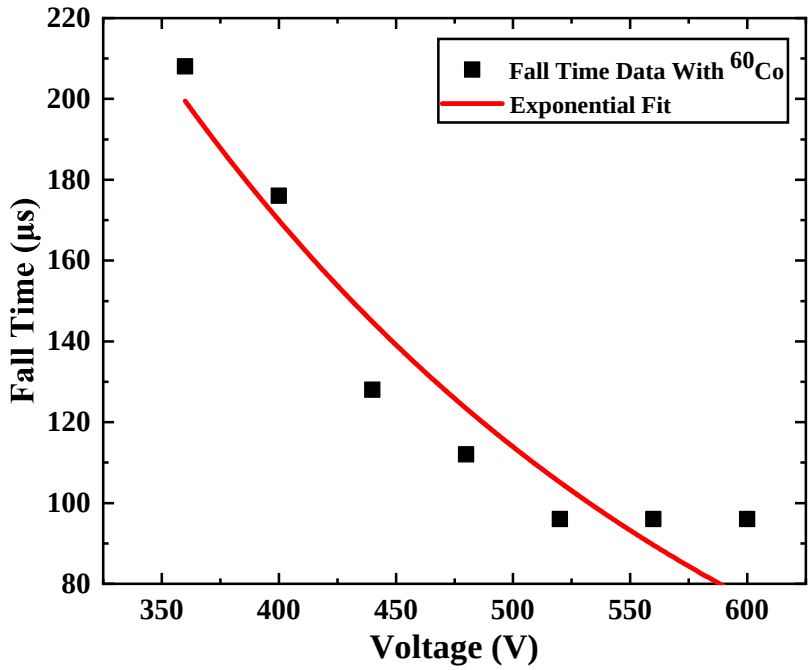


Figure 10: Variation of fall time with applied voltage for the ^{60}Co source. The red line represents the exponential fit to the measured data.

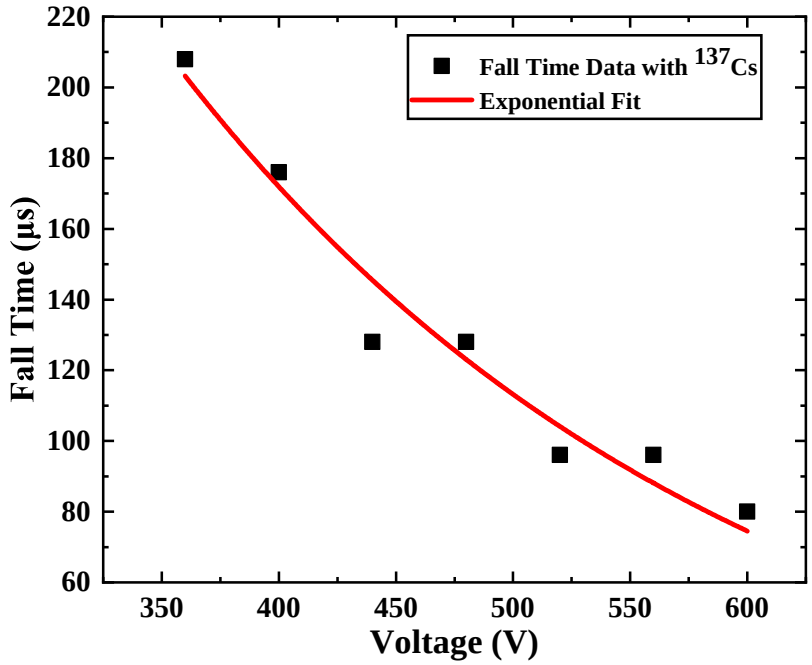


Figure 11: Variation of fall time with applied voltage for the ^{137}Cs source. The red line represents the exponential fit to the measured data.

The fall time data for all three radiation sources exhibit an exponential decrease with increasing applied voltage. Similar to the pulse width behavior, the fall time attains its maximum value at the lowest operating

voltage of 360 V. At low electric field strengths, the collection of charge carriers at the anode is slower, resulting in extended pulse tails and longer fall times. This prolonged charge collection increases the detector dead time, thereby reducing the number of detectable radiation events.

With increasing operating voltage, the electric field inside the GM tube strengthens, leading to faster charge collection and a corresponding reduction in fall time. This reduction allows the detector to recover more rapidly between successive events, thereby improving counting efficiency. The fall time data were fitted using the same exponential function employed for pulse width analysis, and the resulting fit parameters are summarized in Table 2. The extracted exponent values are 0.00507 for background radiation, 0.0040 for the ^{60}Co source, and 0.00418 for the ^{137}Cs source. Although the exponent for background radiation is slightly higher, the overall voltage dependence of fall time remains comparable for all three cases. The exponential model provides a good description of the fall time data for all radiation sources.

Table 2: Best-fit parameters (a and b) obtained from exponential fitting of the pulse fall time as a function of applied voltage for background radiation and the radioactive sources ^{60}Co and ^{137}Cs.

S. No.	Source	a	b
1	Background	1696.00 ± 495.95	0.00507 ± 0.00073
2	^{60}Co	843.29 ± 207.89	0.00400 ± 0.00056
3	^{137}Cs	915.13 ± 161.12	0.00418 ± 0.00040

It is noted that the chosen exponential fitting function is not necessarily unique. However, this functional form was selected based on its successful application in previous studies reported in the literature (Almutairi et al., 2019). The primary objective of the fitting procedure is to highlight the underlying trends in the data; the extracted fit parameters are not used directly for quantitative interpretation of the dead time behavior.

4.4. Relation between Dead Time and Pulse Shape Properties

The relationship between the dead time of the Geiger–Müller (GM) counter and its pulse shape properties–namely fall time, pulse width, and peak-to-peak voltage was systematically examined. Within the investigated operating voltage range, the dead time exhibits an approximately linear dependence on each of these pulse shape parameters. The corresponding correlations between dead time and pulse width, fall time, and peak-to-peak voltage are presented in Figures. 12–14, respectively.

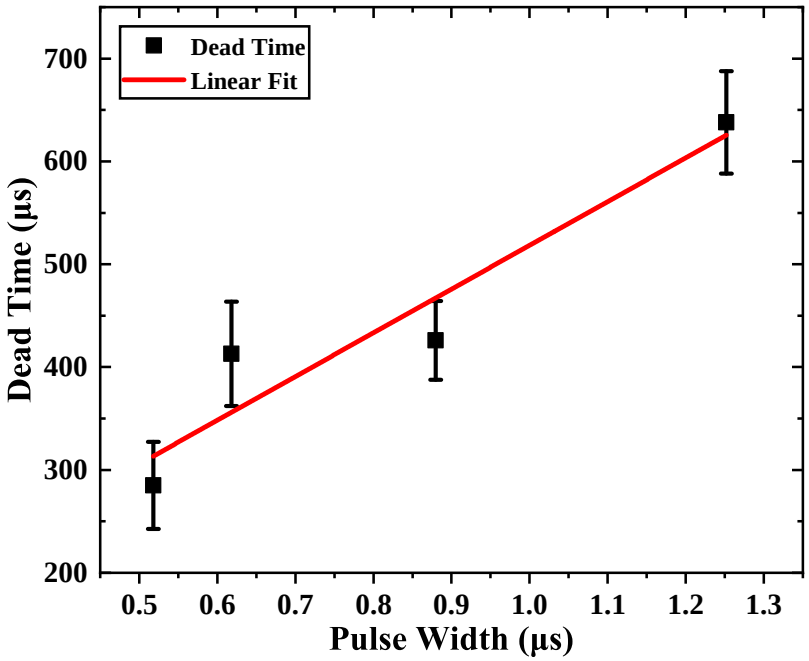


Figure 12: Variation of dead time with pulse width for the ^{137}Cs source showing a linearly increasing trend.

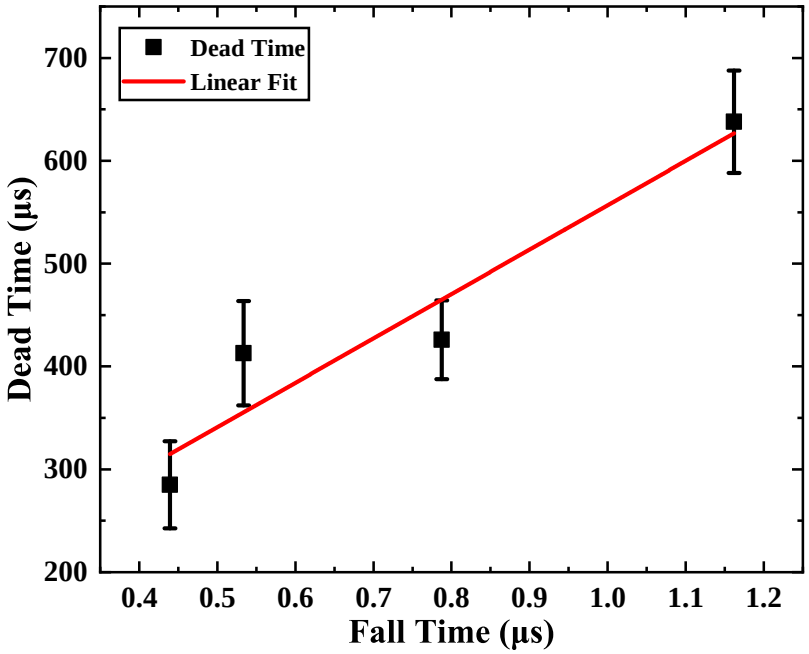


Figure 13: Variation of dead time with fall time for the ^{137}Cs source. The plot shows linear correlation between dead time and fall time.

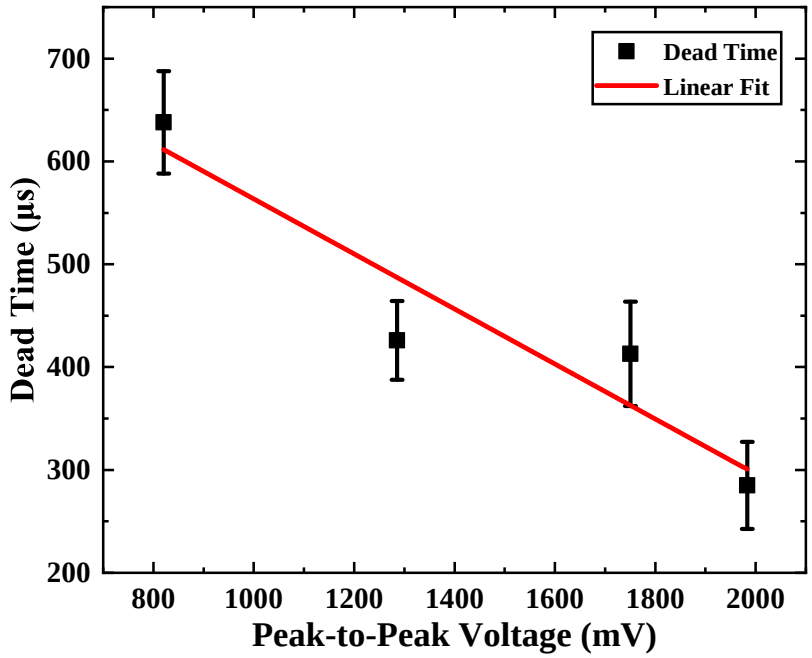


Figure 14: Variation of dead time with peak-to-peak voltage for the ^{137}Cs source. The observed trend indicate the reduction in dead time with increase in peak-to-peak voltage with linear dependence.

The analysis was performed using the ^{137}Cs source, which was also employed for the dead time measurements. At lower applied voltages, the electric field inside the detector is relatively weak, resulting in slower charge collection at the anode. This leads to longer pulse fall times and broader pulse widths, which in turn increase the detector dead time. As the applied voltage increases, enhanced charge collection efficiency produces shorter fall times and narrower pulses, leading to a reduction in dead time.

A clear linear relationship is observed between dead time and fall time, indicating that the detector recovery process is strongly governed by the decay characteristics of the output pulses. The maximum dead time corresponds to conditions where the fall time is longest and the peak-to-peak voltage is lowest. These trends can be attributed to inefficient charge collection and prolonged ion-induced field distortion near the anode at low operating voltages.

It is noted that the observed linear dependence is based on the available dataset within the plateau region. While the present results establish a clear qualitative and quantitative correlation, further measurements over a wider voltage range and with larger datasets could provide additional insight and improve statistical confidence in the observed trends.

5. Conclusions

The experimental results show that the dead time of a Geiger–Müller (GM) counter decreases monotonically with increasing operating voltage within the investigated plateau region. At lower voltages, weaker electric fields lead to slower charge carrier drift and prolonged charge collection, resulting in longer pulse tails and increased dead time. In contrast, higher operating voltages enhance charge collection efficiency, shorten pulse duration, and reduce the dead time.

An approximately linear correlation is observed between dead time and pulse shape parameters, particularly fall time, indicating the important role of pulse decay characteristics in the detector recovery process. Within the studied voltage range, the observed behavior suggests that dead time is governed mainly by voltage-dependent charge collection dynamics rather than by the type of incident radiation.

Overall, the present study provides insight into the recovery characteristics of GM counters under different operating voltages and offers practical guidance for selecting suitable operating conditions to minimize dead time and improve counting performance in radiation measurements.

6. Summary

This work presents a systematic experimental investigation of the pulse shape properties and dead time behavior of a Geiger–Müller (GM) counter as a function of operating voltage. The pulse shape parameters analyzed include pulse width, fall time, and peak-to-peak voltage, measured for ^{60}Co, ^{137}Cs, and background radiation. Dead time measurements were performed within the plateau region using the two-source method under the non-paralyzing model assumption.

The results show that pulse width and fall time decrease exponentially with increasing applied voltage, while the peak-to-peak voltage increases approximately linearly. These trends are attributed to enhanced gas multiplication and faster charge collection at higher electric field strengths. The voltage dependence of the pulse shape parameters is found to be similar for all radiation sources studied, indicating a weak dependence on the nature and energy of the incident radiation. Additionally, the comparable exponential parameters obtained for pulse width and fall time suggest a similar voltage dependence of the main pulse structure and the pulse decay tail.

An approximately linear correlation between dead time and pulse shape characteristics is observed, with dead time exhibiting a linear dependence on pulse width, fall time, and peak-to-peak voltage within the investigated voltage range.

References

Akyurek, T., Yousaf, M., Liu, X., & Usman, S. (2015). Gm counter dead time dependence on applied voltage, operating temperature and fatigue. *Progress in Nuclear Energy*, *73*, 26–35.

Almutairi, B., Akyurek, T., & Usman, S. (2019). Voltage-dependent pulse shape analysis of geiger–müller counter. *Nuclear Engineering and Technology*, *51*, 1081–1090.

Almutairi, B., Alam, S., Akyurek, T., Goodwin, C. S., & Usman, S. (2020). Experimental evaluation of the dead time phenomenon for gm detector: Dead time dependence on operating voltage. *Scientific Reports*, *10*, 19955.

Almutairi, B., Alam, S., Goodwin, C. S., Usman, S., & Akyurek, T. (2021). Simultaneous experimental evaluation of pulse shape and dead time phenomenon of gm detector. *Scientific Reports*, *11*, 3320.

Evans, R. D. (1955). *The atomic nucleus*. New York: McGraw–Hill.

Feller, W. (1948). On probability problems in the theory of counters. In *Studies and essays presented to r. courant on his 60th birthday* (pp. 105–115). New York: Interscience.

Geiger, H., Müller, W., et al. (1928). Das elektronenzählrohr. *Physikalische Zeitschrift*, *29*, 839–841.

Knoll, G. F. (2010). *Radiation detection and measurement* (4th ed.). New York: John Wiley & Sons.

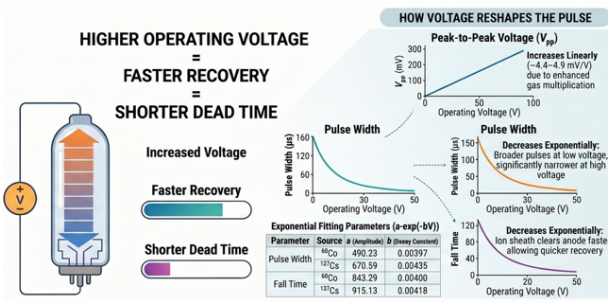
Lee, S. H., & Gardner, R. P. (2000). A new geiger–müller counter dead time model. *Applied Radiation and Isotopes*, *53*, 731–737.

Müller, J. W. (1973). Dead-time problems. *Nuclear Instruments and Methods*, *112*, 47–57.

Patil, A., & Usman, S. (2009). Measurement and application of paralysis factor for improved detector dead time characterization. *Nuclear Technology*, *165*, 249–256.

Stever, H. G. (1942). The discharge mechanism of fast geiger–müller counters from dead-time experiments. *Physical Review*, *61*, 38–45.

Graphical Abstract



Mr. Vikas Kumar: A Kurukshetra University alumnus (M.Sc. Physics), Vikas is currently advancing his research as a doctoral candidate at IIT Mandi.

Mr. Ankit Kumar: Following his M.Sc. in Physics from Kurukshetra University, Ankit moved on to pursue his Ph.D. at the University of Delhi.

Mr. Aryan: After completing his M.Sc. in Physics at Kurukshetra University, Aryan stepped in to spearhead the data and technical analysis for the project.

Dr. Vikas: Having successfully completed his doctorate, Vikas now teaches in Delhi. He was instrumental in refining the overall analysis and polishing the final manuscript draft.

Dr. Hardev Singh: A faculty member in the Department of Physics at Kurukshetra University, He provided the overall supervision and publication oversight for the project.
